The effect of sorbent regeneration enthalpy on the performance of the novel Swing Adsorption Reactor Cluster (SARC) for post-combustion CO_2 capture

*Schalk Cloete[1], Antonio Giuffrida[2], Matteo C. Romano[2] & Abdelghafour Zaabout[1]**

[1] SINTEF Industry, Trondheim, Norway

[2] Department of Energy, Politecnico di Milano, Milan, Italy

*Corresponding author:

Dr. Abdelghafour Zaabout

Flow Technology Group

SINTEF Industry

S.P. Andersens vei 15 B

7031 Trondheim, Norway

Phone: +47 93008204

Email: abdelghafour.zaabout@sintef.no

Abstract

The recently proposed SARC concept combines a temperature swing and a vacuum swing to efficiently regenerate a CO_2 capture sorbent. A heat pump is used to facilitate the temperature swing by transferring heat from the exothermic carbonation to the endothermic regeneration reaction. This study uses combined reactor and power plant simulations to investigate an interesting trade-off presented by the SARC concept: sorbents with higher regeneration enthalpies will require more heat transfer between carbonation and regeneration, but also allow for a smaller temperature swing, thus enabling the heat pump to transfer this heat more efficiently. Studies showed that the optimal process efficiency is achieved at a sorbent regeneration enthalpy in the range of 100-150 kJ/mol, thus avoiding the need for novel sorbents with very low regeneration enthalpies. Simulation results also highlighted another interesting feature of the SARC concept: the generally undesired adsorption of water vapour by the sorbent does not reduce the overall SARC efficiency because the release of water vapour under regeneration enhances the pressure swing. Finally, a central composite design was conducted to fully understand the SARC behaviour when using sorbents with different regeneration enthalpies. These insights are important for optimal sorbent selection for the SARC concept in future studies.

Keywords: SARC, pressure swing, temperature swing, CO_2 capture, energy penalty.

1 Introduction

CO_2 capture and storage (CCS) has a critical role to play in achieving the "beyond 2 °C" goal of the Paris Climate accord [1]. The latest IPCC report showed that most models simply could not achieve stringent CO_2 reductions without CCS, while the few model runs that did achieve the scenarios showed a median 140% increase in total cost [2].

CO_2 capture is generally the most expensive component of CCS, primarily due to the energy penalty imposed on the host system – 7-12 %-points with state of the art technologies in coal-fired power plants [3-5]. Energy penalty reduction is therefore a key objective of CO_2 capture research and the development of new process concepts.

Among the three main categories of CO_2 capture, post-combustion capture is the most versatile with amine scrubbing being the most developed [4, 5]. It can be applied to any process generating a flue gas stream containing significant concentrations of CO_2, making it ideally suited to retrofits and industrial applications. Low temperature adsorption-based CO_2 capture technologies are receiving increased interest due to the potential to further decrease the energy penalty compared to benchmark technologies [6]. These processes can operate under different modes cycling vacuum/pressure swing (VSA/PSA) [7, 8] or temperature swing (TSA) [9] over a sorbent, depending on the type of the sorbent. In general, VSA/PSA systems are suited to physisorption while TSA systems are more suited to chemisorption. The latter has high CO_2 adsorption capacity and selectivity, in addition to high tolerance to water [6]. However, their high regeneration enthalpies result in high energy penalty [10].

Recent research on this technology has focussed on finding alternatives to the conventional interconnected fluidized bed configuration where the sorbent is circulating between two reactors operating at different temperatures [11, 12]. In this configuration, multistage co- and counter- current risers have been proposed and tested to increase the adsorption working capacity of the sorbent, thereby reducing the sorbent circulation rate [13-15]. Other reactor configurations considered reducing the overall energy penalty through heat integration. This includes, the moving bed [16], the

inter-stage heat integration interconnected fluidized bed [10] and the Swing Adsorption Reactor Cluster (SARC) [17]. The latter is a new post-combustion capture concept, aiming to significantly reduce the energy penalty related to CCS, while simultaneously simplifying the retrofitting process.

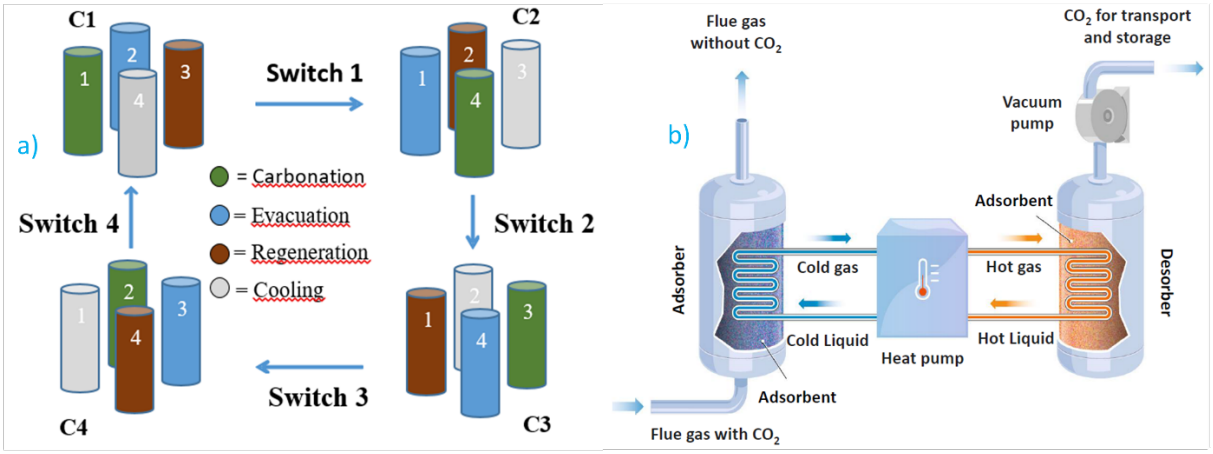

Figure 1: SARC conceptual design: a) a cluster of SARC reactors for continuous gas stream processing; b) SARC working principle showing heat transfer from a reactor under carbonation to one under regeneration using a heat pump.

The SARC concept combines vacuum swing using a vacuum pump and temperature swing using a heat pump to regenerate the sorbent (Figure 1.b). A cluster of standalone bubbling fluidized bed reactors is used to accommodate the vacuum swing and enable processing of a steady incoming flue gas stream (Figure 1.a)). Combining vacuum and temperature swings in this manner facilitates a small temperature difference between carbonation and regeneration, thus allowing the heat pump to transfer the heat from carbonation to regeneration with a very high coefficient of performance. Given that the process uses only electricity and does not require steam extraction from the power cycle, retrofitting is simplified and large efficiency gains are possible in industrial processes where large quantities of steam are not available.

To minimize the energy penalty of CO_2 capture, low regeneration enthalpy has long been the primary objective in CO_2 capture sorbent/solvent development. For example, a review by Goto, Yogo [18] found that the overall energy penalty of post-combustion CO_2 capture from coal-fired power plants reduces by 2 %-points for every 1 MJ/t-CO_2 reduction in regeneration energy requirement. It is noted, however, that the regeneration energy requirement does not depend only on the regeneration enthalpy, but also on the sensible heat content and the degree of heat integration between the sorbent streams exiting the two reactors. In addition, the total energy penalty depends not only on the regeneration energy requirement, but also on the temperature at which regeneration heat is required.

Oexmann and Kather [19] illustrated the point that regeneration enthalpy is not the only factor influencing the regeneration duty in wet chemical absorption systems. Sensible heat and water evaporation enthalpy are also important factors and should be included in the analysis because of dependencies on the regeneration enthalpy. Other aspects such as reaction kinetics and CO_2 capture capacity are also important elements to consider. van Nierop, Hormoz [20] showed that temperature swing CO_2 capture processes generally benefit from lower regeneration enthalpy solvents, but that solvent flowrates and flue gas cooling requirements can become prohibitive at regeneration enthalpies below that of MEA (80 kJ/mol).

The SARC concept presents a different dynamic related to changes in regeneration enthalpy. Sorbents with a higher regeneration enthalpy are more sensitive to temperature, thus lowering the temperature swing required to achieve a given sorbent utilization. Thus, even though such a sorbent will require more heat during regeneration, the smaller temperature swing will allow the heat pump to supply this heat more efficiently, creating an interesting trade-off for overall process efficiency. This feature could allow the SARC concept to benefit from proven low-cost sorbents that have fallen out of favour due to relatively high regeneration enthalpies (e.g. potassium [11, 21, 22] or sodium [23] carbonates).

In addition, sorbents for post-combustion CO_2 capture tend to adsorb water vapour present in the flue gas, imposing a significant additional energy penalty [24]. In the SARC concept, the desorption of previously adsorbed water vapour in the regeneration reactor reduces the CO_2 partial pressure, thus contributing to the pressure swing of the process. This increased pressure swing then allows for a smaller temperature swing to achieve a given sorbent utilization, increasing the heat pump efficiency. Water vapour adsorption thus presents another interesting trade-off in the SARC concept: larger regeneration energy requirement in exchange for more efficient heat transfer through the heat pump.

This study will quantify the effect of sorbent regeneration enthalpy and water vapour adsorption on the overall efficiency of a coal-fired power plant with post-combustion CO_2 capture using SARC.

2 Reactor and power plant simulations

The SARC reactor was simulated as a series of four CSTRs, similar to the previous work of the authors [17]. The only differences are the CO_2 adsorption isotherm employed, the sizing of the reactors and heat transfer tubes, and the duration of the four steps in the transient SARC cycle. These three changes to the previous reactor simulations are described in more detail below, while readers are referred to the aforementioned work [17] for the complete model description.

2.1 CO_2 adsorption isotherm

To assess the impact of the sorbent regeneration enthalpy on the process performance, a simple hypothetical CO_2 adsorption isotherm is defined according to the Langmuir model.

$$\frac{q}{q_{sat}} = \frac{b(T)p_{CO_2}}{1 + b(T)p_{CO_2}} \qquad \text{Equation 1}$$

$$b(T) = b_0 \exp\left(\frac{dH}{RT}\right) \qquad \text{Equation 2}$$

Here, q [mol/kg] is the molar CO_2 loading of per unit mass of sorbent and q_{sat} is the maximum achievable solid loading (assumed to be 2.65 mol/kg). p_{CO_2} [bar] is the CO_2 partial pressure, T [K] is the temperature, and R [8.314 J/mol.K] is the ideal gas constant.

The adsorption enthalpy, dH [J/mol], and the pre-exponential factor, b_0 [1/bar], are modified in this work to investigate four different adsorption enthalpies: 50, 100, 150 and 200 kJ/mol. For each selected adsorption enthalpy, the pre-exponential factor was calculated to return $q/q_{sat} = 0.5$ if $p_{CO_2} = 0.01$ bar at $T = 333$ K. This condition represents approximately 90% CO_2 capture from a coal-fired power plant (flue gas $p_{CO_2} \approx 0.13$) when adsorption is carried out at 333 K. In other words, when

$q/q_{sat} = 0.5$, about 0.01/0.13 = 8% of the CO_2 in the flue gas will slip through without being adsorbed under the assumption that the reactor is large and chemical equilibrium is reached.

The four hypothetical isotherms are visualized in Figure 2, where it is immediately evident that higher regeneration enthalpies result in a higher temperature sensitivity. Note that the isotherm at 333 K (the carbonation temperature) is identical for all four isotherms, providing an effective basis for standardization to evaluate the effect of the added temperature sensitivity at higher regeneration enthalpies. It was explicitly confirmed that the required temperature swing calculated by the reactor model is not sensitive to the selected value of q/q_{sat} at $p_{CO_2} = 0.01$ bar.

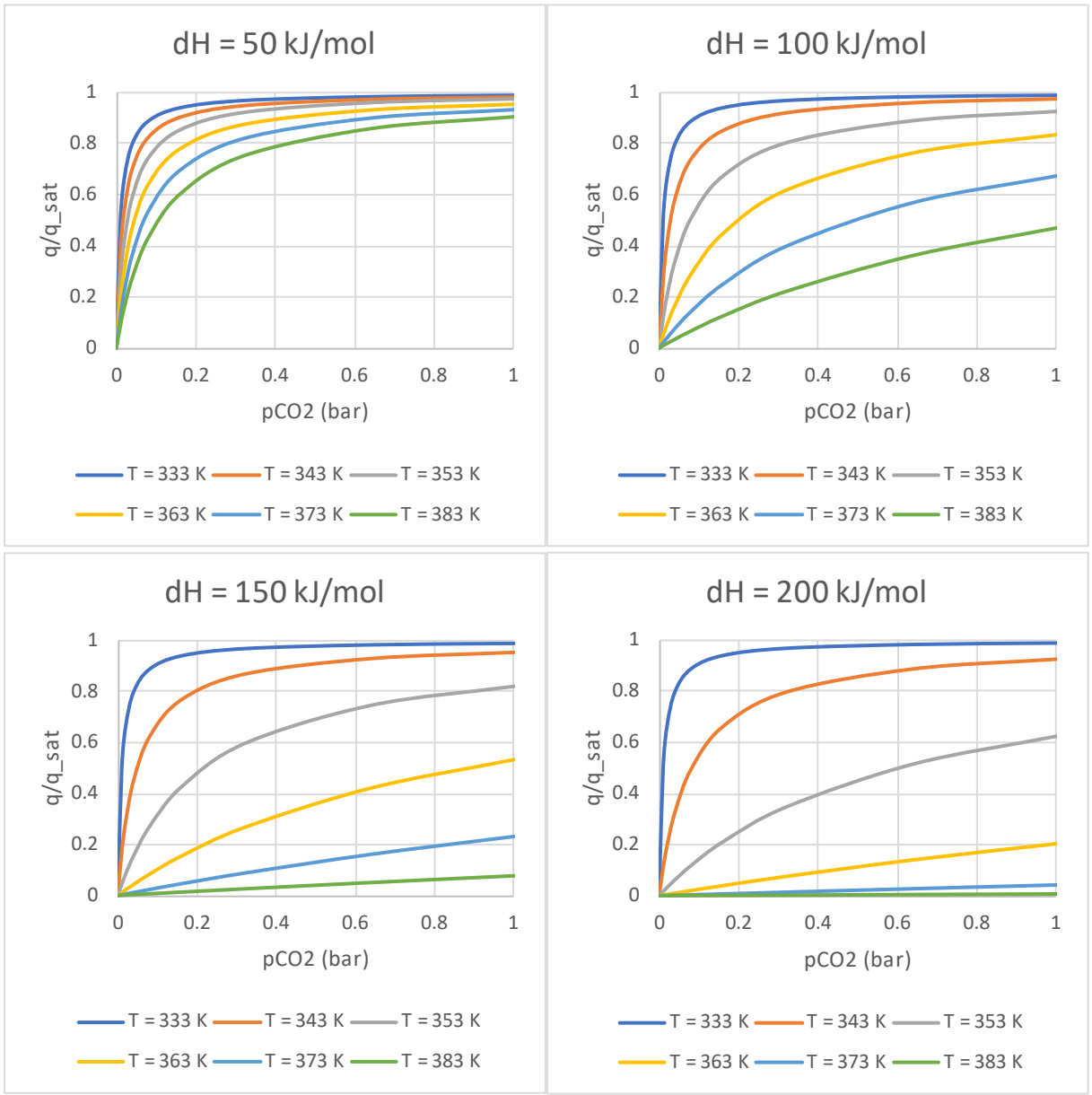

Figure 2: Hypothetical CO_2 adsorption isotherms for four different regeneration enthalpies investigated.

For the cases that included water vapour adsorption, the same water vapour adsorption isotherm from the previous work [17] was employed. This isotherm was measured for a supported amine sorbent in the work of Veneman, Frigka [24] and will be employed to draw a general conclusion about the effect

of water adsorption in this study. It is noted, however, that the shape of the water vapour adsorption isotherm for different sorbents can also have a significant influence on the process performance.

2.2 Reactor and heat transfer tube sizing

All simulations used a reactor that is 4.85 m in diameter. At a fluidization velocity of 1 m/s, 100 such reactors are required to process the 610 Nm^3/s flue gas stream from the coal-fired power plant. It was assumed that these 100 reactors are separated into 4 clusters of 25 reactors each. The next section will describe the distribution of these 25 reactors between the four different steps in the SARC cycle.

Two reactor heights were considered: 5 m and 10 m. This was done to investigate the trade-off between the extra heat transfer area and the increased pressure drop in a taller reactor.

As in the previous work [17], the heat transfer tube bundle was assumed to occupy the space of the static bed, with an additional 80% of space afforded for bed expansion. Thus, the tube bundle occupied 100/(100+80)=56% of the reactor height. This study used thinner tubes than the previous work to maximize the heat transfer area in the bed. The square tube bundle was assumed to consist of 6 mm tubes, arranged in a staggered configuration with a pitch of 9 mm.

Another important change from the previous study was the inclusion of added thermal mass of the tubes and the reactor body in the simulation. Wall thicknesses of the reactor and tubes were assumed to be 20 mm and 0.4 mm respectively. The assumed construction material is steel with a density of 8050 kg/m^3 and a heat capacity of 0.5 kJ/kg.K.

2.3 The SARC cycle

As thoroughly explained in Section 4.2 of the previous study by the authors [17], the SARC cycle consists of four steps (see Figure 4 in this study for a graphical example of the SARC cycle):

1. Carbonation. Flue gas is fed to the reactor and the sorbent adsorbs CO_2 and H_2O with continuous heat extraction by the heat pump to maintain a near-constant reactor temperature.
2. Evacuation. Gas is extracted from the reactor to minimize the N_2 in the reactor at the start of the regeneration stage. This is necessary to maximize the CO_2 purity.
3. Regeneration. The vacuum pump reduces the reactor pressure to 0.1 bar, while the heat pump adds heat to the reactor. This combined pressure and vacuum swing releases CO_2 and H_2O from the sorbent, while the reactor temperature continuously increases.
4. Cooling. Before the start of the next carbonation step, the reactor temperature must be reduced to a suitable level to achieve a high degree of CO_2 capture.

An increase in the regeneration enthalpy of the hypothetical sorbent described in Section 2.1 increases the required heat transfer from carbonation to regeneration, but also reduces the required temperature difference between carbonation and regeneration. Given that the heat transfer area in the reactor is kept constant over all the different cases, the cooling step must be longer for the case with low regeneration enthalpy to achieve the larger temperature swing.

Thus, the distribution of reactors between regeneration and cooling was altered for each case to ensure that the reactor is successfully cooled to the carbonation temperature. In each cluster of 25 reactors, 10 reactors were always in the carbonation step, 1 reactor in the evacuation step, and the

remaining 14 reactors distributed between regeneration and cooling. Figure 4 discussed in Section 3.1 provides a graphical illustration of this practice.

2.4 Power plant simulations

The flowsheet of the coal-fired power plant integrated with the SARC process is shown in Figure 3. The power plant is based on a 270/60 bar and 600/620°C ultra-supercritical reheated steam cycle. Flue gas from the wet limestone desulphurizer (FGD) are blown to the absorber (carbonator) and then emitted to the stack. Sorbent is regenerated releasing low-pressure CO_2, which is compressed to 1 bar by the vacuum pump and then in a 3-intercooled stage compressor train to 80 bar before liquefaction and final pumping to 110 bar.

The ammonia heat pump features a simple vapor compression cycle driven by a single-stage compressor with isentropic and electric-mechanical efficiencies of 85 and 94% respectively. Heat integration between the steam cycle and the CO_2 capture process involves the heat recovery from ammonia de-superheating and CO_2 compressors intercoolers. This low temperature heat is recovered by preheating the condensate (streams #21 and 22 in Figure 3), which allows deactivating the first two feedwater heaters of the steam cycle and ultimately increasing the plant power output and efficiency.

The power plant simulations are carried out with exactly the same methodology as outlined in the previous work [17], where a comprehensive description of the plant and the complete list of calculation assumptions is reported.

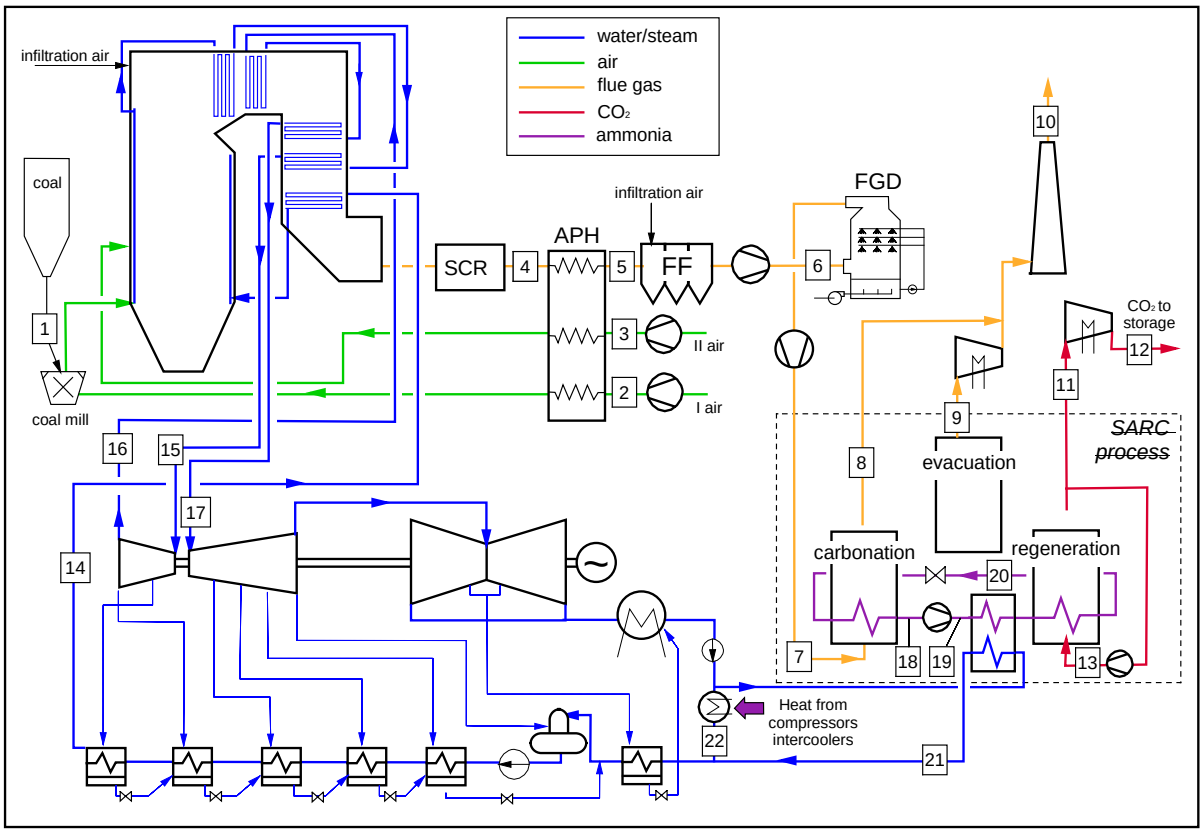

Figure 3: Flowsheet of the coal power plant with CO_2 capture with the SARC process served by an ammonia heat pump.

3 Results and discussion

Results will be presented in four sections: 1) the effect of regeneration enthalpy on the SARC reactor behaviour, 2) the effect of increasing the reactor height, 3) the effect of including water vapour adsorption, and 4) a 3-factor parametric study investigating the response of plant efficiency to changes in regeneration enthalpy, evacuation pressure and cycle length.

3.1 The effect of regeneration enthalpy on the SARC cycle

As outlined in Section 2.1, an increase in regeneration enthalpy requires more heat transfer from carbonation to regeneration, but allows for an increased heat pump efficiency due to a smaller temperature swing. Figure 4 shows a practical illustration of this effect.

The first notable trend is the decrease in the required temperature swing with an increase in regeneration enthalpy. This not only increases the heat pump efficiency, but also limits the sensible heat transfer required to heat the bed during regeneration and cool it during cooling. The temperature swing is especially large for the 50 kJ/mol regeneration enthalpy, so a large heat pump power consumption may be expected for this case.

Secondly, the carbonation temperature in the reactor increases with an increase in regeneration enthalpy. This effect is caused by the larger rate of heat extraction required over the constant heat transfer surface area with a constant temperature heat pump working fluid (328 K). Since the heat pump efficiency is determined by the difference between the evaporation and condensation temperatures of the working fluid, an increased temperature difference between the reactor and the working fluid will significantly decrease heat pump efficiency.

Thirdly, the longer cooling time required in the cases with lower regeneration enthalpy is visible in Figure 4. As outlined in Section 2.3, this longer time is required to allow the reactor to reach a sufficiently low temperature for efficient CO_2 capture. To maintain a constant number of reactors in the cluster, the longer cooling time reduces the time allowed for sorbent regeneration. However, the low regeneration enthalpy allows the temperature to rise rapidly under regeneration, causing the reactor temperature to approach the heat pump condensation temperature by the end of the regeneration stage. The shorter regeneration stage therefore does not negatively affect heat pump efficiency. This was confirmed by doubling the regeneration time for the 50 kJ/mol regeneration enthalpy case. The required heat pump temperature difference decreased by only 0.5 K in this case.

Also note that flue gas is fed during the cooling stage at 10% the flowrate during carbonation [17] to ensure that the reactor remains fluidized while it is being cooled. When the cooling stage becomes long enough, the flue gas has enough time to rise all the way through the multistage fluidized bed, allowing N_2 and H_2O to reach the reactor outlet. This flue gas breakthrough during cooling is clearly observed in the 50 kJ/mol case in Figure 4.

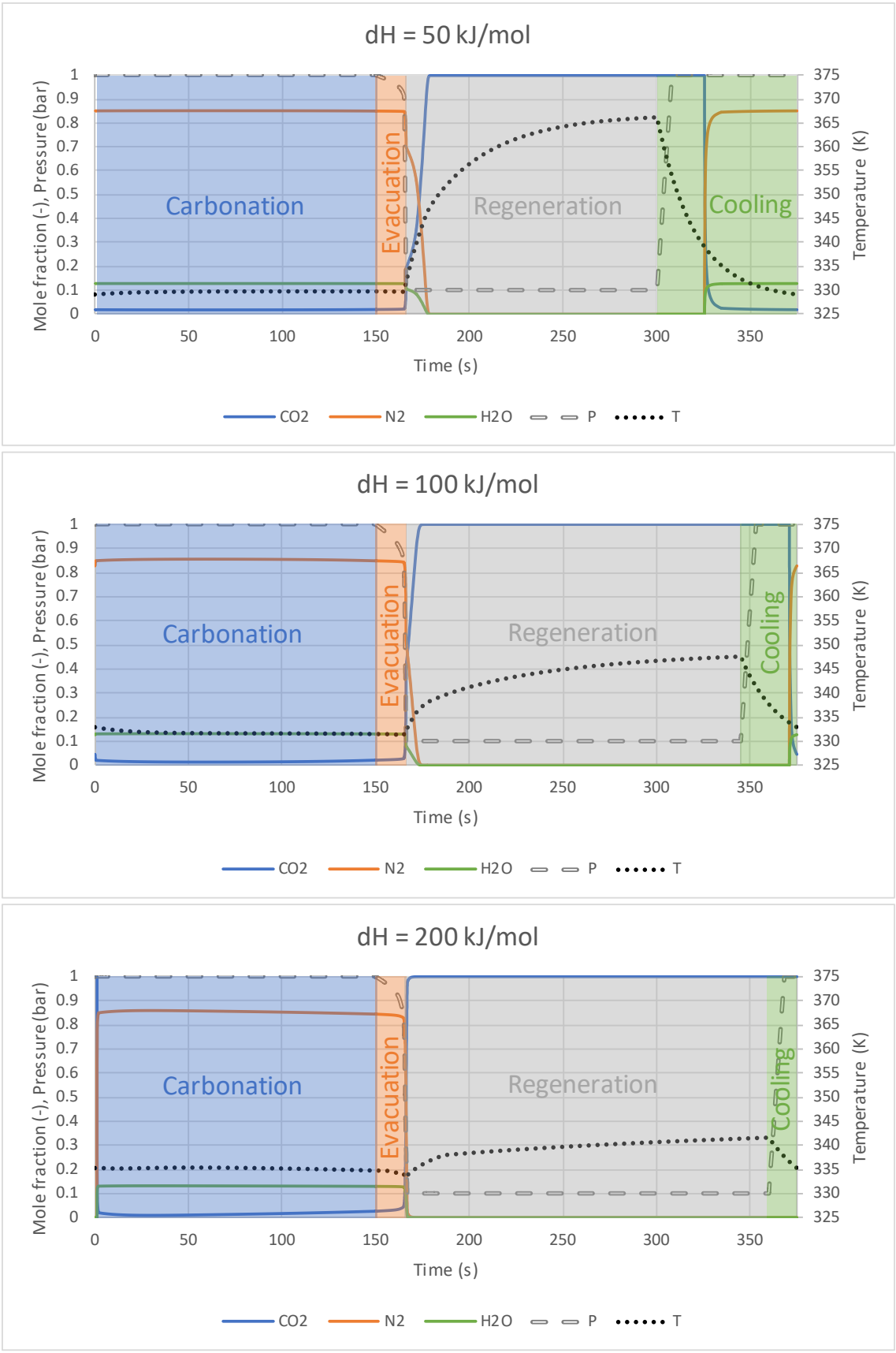

Figure 4: Gas species mole fractions, reactor pressure and reactor temperature over one SARC cycle for three different reaction enthalpies. The simulated reactor height was 5 m and no water vapour adsorption was included.

When adding all these effects together, the total energy penalty trend in Figure 5 emerges. As expected, the heat pump consumption is the only component showing significant changes between the four cases. For the lowest regeneration enthalpy (50 kJ/mol), the large temperature swing required imposed a very large heat pump consumption. Figure 5 (right) shows that the difference between the heat pump condensation and regeneration temperatures is much larger than the other cases, but also that, despite the low reaction enthalpy, the total heat transfer requirement is relatively large. This is due to the large amount of energy that must be transferred to heat and cool the sorbent and reactor over the cycle.

Coal combustion generates about 455 kJ of heat per mol of released CO_2. Regeneration reaction heat requirements for 90% CO_2 capture will therefore range from $90\% \times 50/455 = 10\%$ to $90\% \times 200/455 = 40\%$ of LHV fuel input for the cases considered in this study. It is therefore clear from Figure 5 (right) that total heat transfer requirement is mainly sensible heat for the 50 kJ/mol case and mainly regeneration reaction heat for the 200 kJ/mol case.

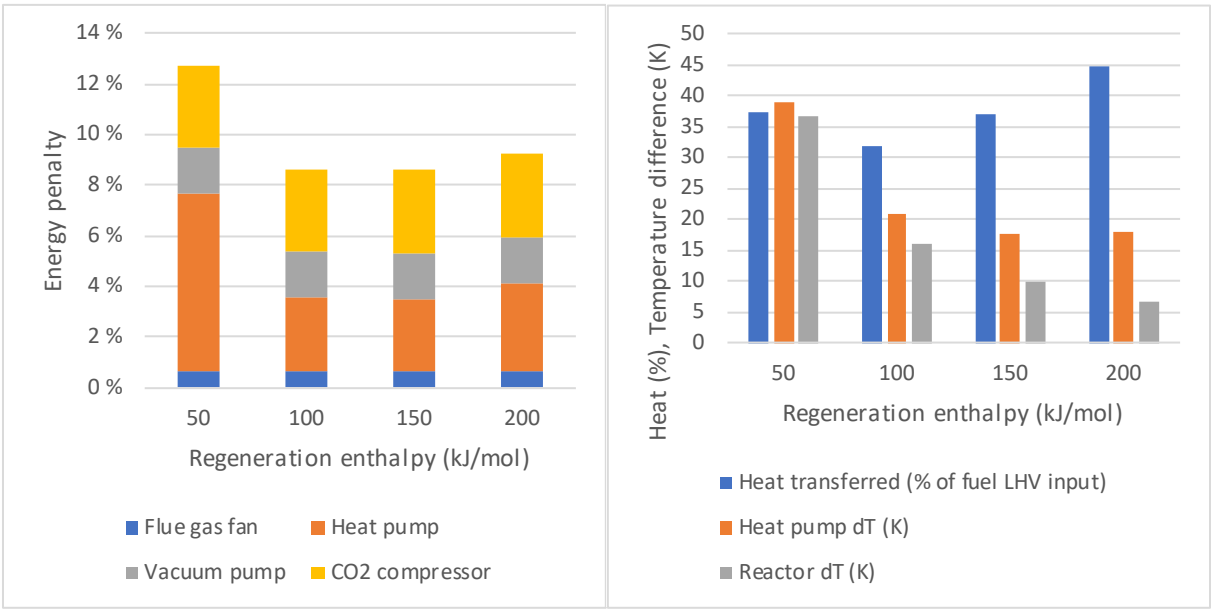

Figure 5: Power plant simulation outputs for the four different regeneration enthalpies in the 5 m reactor. Left: Energy penalty breakdown as a percentage of LHV fuel input. Right: The heat transferred by the heat pump as a percentage of total LHV fuel input to the plant, the difference between the condensation and evaporation temperatures of the heat pump working fluid, and the difference between the average reactor temperatures at the end of the regeneration and carbonation stages. More details are available in Table A 1 in the appendix.

On the other hand, the highest regeneration enthalpy (200 kJ/mol) also increased the heat pump consumption due to the large amount of reaction heat to be transferred and the substantial temperature difference between the heat pump working fluid and the bed material required to achieve the required heat transfer rate. Due to the latter effect, Figure 5 (right) shows that the difference between the condensation and regeneration temperatures in the heat pump did not improve when moving from the 150 kJ/mol case to the 200 kJ/mol case, although the required temperature swing in the reactor continued to decrease. This indicates that energy benefits may be obtained with sorbents with high regeneration enthalpy by increasing the heat transfer surface and the cycle time, which would reduce the heat pump dT to values closer to the reactor dT.

The cases with 100 kJ/mol and 150 kJ/mol achieved the optimal performance between these two extremes. Figure 5 (right) shows the trade-off between total heat transfer and the heat pump temperature difference (inversely proportional to heat pump efficiency) for these two cases, resulting in similar heat pump power consumption shown in Figure 5 (left).

Finally, when comparing Figure 5 (left) and Table A 1, results show that the overall energy penalty is about 0.4 %-points lower than the direct energy penalty from the SARC reactors and CO_2 compression. For example, Table A 1 shows that the overall plant energy penalty is 8.16 %-points for the 150 kJ/mol case, while the total power consumption for this case in Figure 5 (left) is 8.58 %-points. This small difference is due to some heat recovery from the compressors and vacuum pump.

3.2 The effect of reactor height

Doubling the reactor height doubles the available heat transfer area inside the reactor, but also doubles the reactor pressure drop. By comparing Figure 6 (left) to Figure 5 (left), this trade-off can be clearly identified: the taller reactor shows a lower heat pump consumption at the cost of more consumption from the fan driving the flue gas through the reactors.

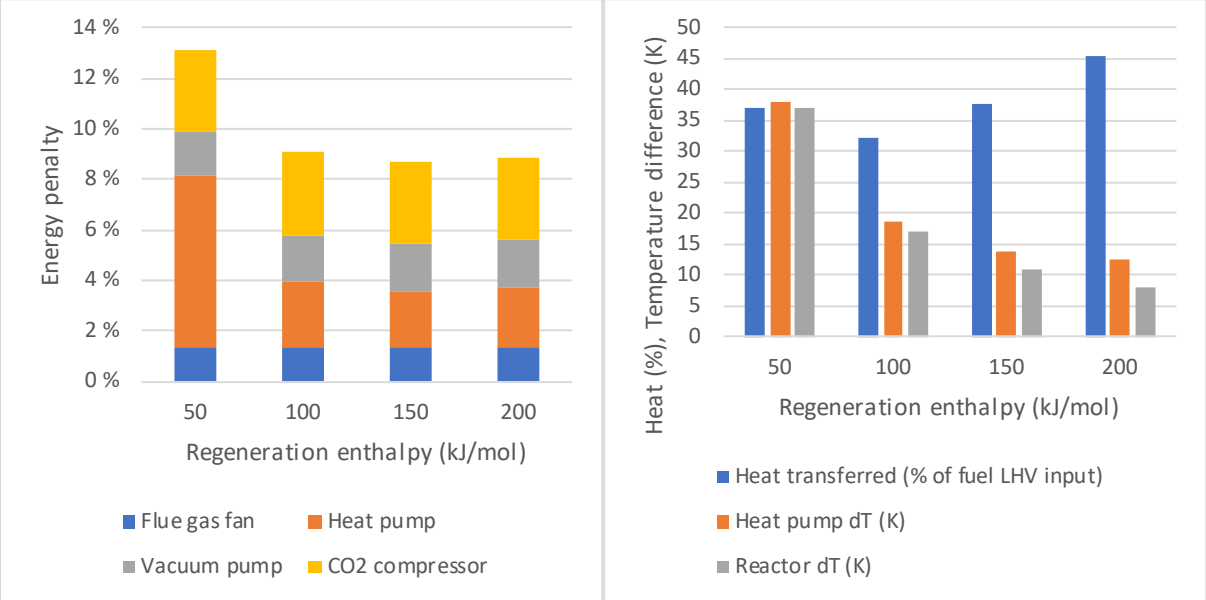

Figure 6: Power plant simulation outputs for the four different regeneration enthalpies in the 10 m reactor. Left: Energy penalty breakdown as a percentage of LHV fuel input. Right: The heat transferred by the heat pump as a percentage of total LHV fuel input to the plant, the difference between the condensation and evaporation temperatures of the heat pump working fluid, and the difference between the average reactor temperatures at the end of the regeneration and carbonation stages. More details are available in Table A 2 in the appendix.

In general, only subtle changes are observed in the overall energy penalty. As expected, the increased heat transfer surface area in the taller reactor shifted the optimal point towards the higher regeneration enthalpies. This is better observed in Figure 6 (right) where the difference between condensation and regeneration temperatures in the heat pump keep decreasing with increasing regeneration enthalpy. The temperature difference between the reactor and the heat pump working fluid is halved when the heat transfer surface area is doubled, thus reducing this negative effect on heat pump efficiency at high regeneration enthalpies. This can be seen from the much smaller difference between the heat pump dT and the reactor dT in Figure 6 (right) relative to Figure 5 (right).

3.3 The effect of water vapour adsorption

The simulations presented in this section enabled water vapour adsorption according to the adsorption isotherm described in the previous work [17] with an adsorption enthalpy of 43 kJ/mol [24]. Inclusion of water vapour adsorption and desorption is illustrated in the comparative SARC cycles displayed in Figure 7. The presence of water vapour in the regeneration step reduces the CO_2 partial pressure, thus allowing for a smaller temperature swing.

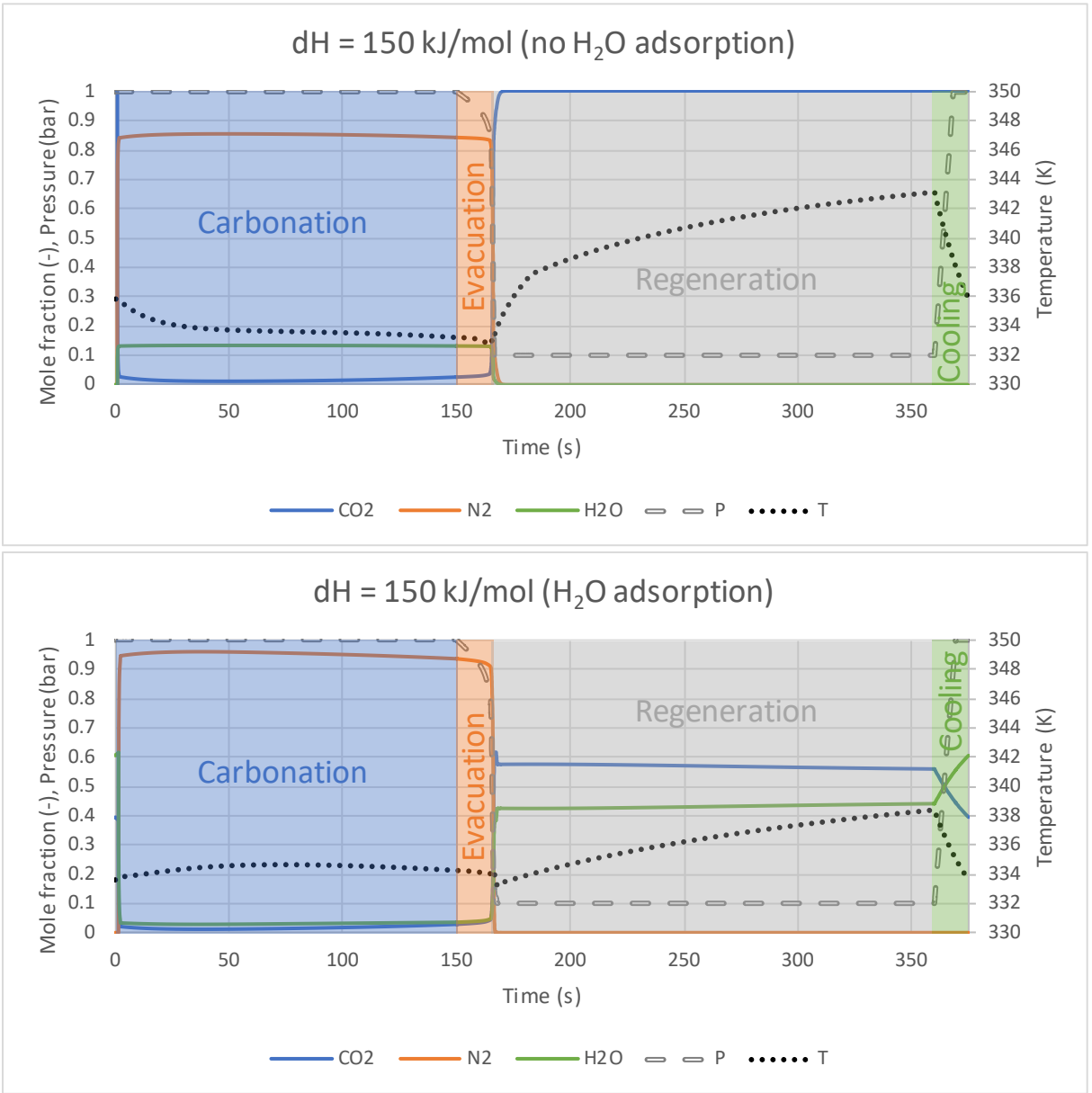

Figure 7: Gas species mole fractions, reactor pressure and reactor temperature over one SARC cycle for cases with and without water vapour adsorption. The simulated reactor height was 5 m.

The power plant performance is illustrated in Figure 8. In comparison to Figure 5, the biggest difference is the substantial reduction in the overall energy penalty of the 50 kJ/mol case. The added partial pressure swing facilitated by the desorption of water vapour allowed for a much smaller temperature swing, thus substantially reducing the large heat pump consumption displayed in Figure 5.

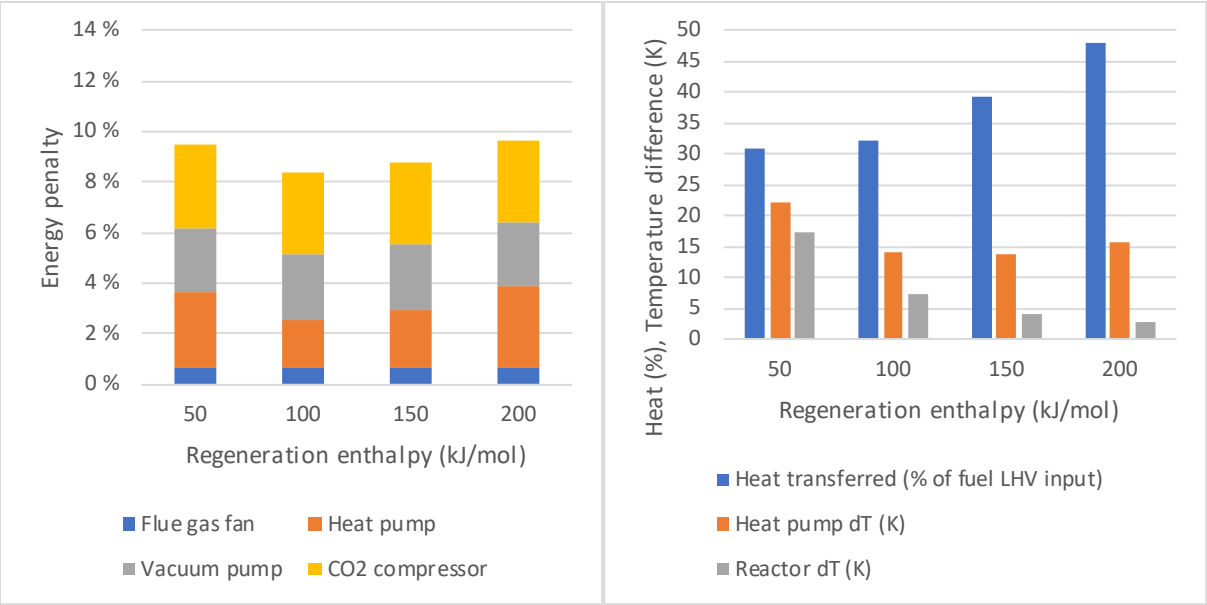

Figure 8: Power plant simulation outputs for the four different regeneration enthalpies in the 5 m reactor with water vapour adsorption included. Left: Energy penalty breakdown as a percentage of LHV fuel input. Right: The heat transferred by the heat pump as a percentage of total LHV fuel input to the plant, the difference between the condensation and evaporation temperatures of the heat pump working fluid, and the difference between the average reactor temperatures at the end of the regeneration and carbonation stages. More details are available in Table A 3 in the appendix.

The second clear difference between Figure 8 (left) and Figure 5 (left) is a decrease in heat pump consumption, but a similarly large increase in vacuum pump consumption. The added partial pressure swing reduced the required temperature difference, thus reducing heat pump consumption despite the increase in required heat transfer from the water vapour adsorption enthalpy. However, the release of water vapour in the regeneration stage also increased the volume of gas to be extracted through the vacuum pump, thus increasing its consumption.

Thirdly, the optimal operating point shifted slightly to the lower reaction enthalpies. This is due to the decrease in required temperature swing and the added reaction enthalpy of water vapour adsorption that increase the relative importance of the temperature difference between the reactor and the heat pump working fluid. As this required temperature difference increases with CO_2 adsorption enthalpy, the difference between heat pump condensation and regeneration temperatures actually increases from the 150 kJ/mol to the 200 kJ/mol case in Figure 8 (right), even though the reactor temperature swing continues to decrease. This is due to the increased temperature difference between the reactor and the heat pump working fluid that is required to increase the heat transfer rate over the constant surface area of the heat transfer tubes in the 200 kJ/mol case.

3.4 Parametric study

This final section will present a 3-factor central composite design [25] on the case investigated in the previous section (5 m reactor with water vapour adsorption) to give more insight into the behaviour of the SARC process. Details of the cases included in the central composite design can be viewed in Table A 4 in the Appendix.

Central composite designs quantify the response of certain dependent variables (e.g. the energy penalty), to changes in selected independent variables (generally called factors). This response is

quantified by a second order polynomial, which provides insight into the nature of the response and can predict the response at different locations within or even slightly outside the parameter space. Each factor is evaluated across 5 levels. The three factors selected for this study are outlined below:

1. Regeneration enthalpy was investigated at the levels of 41, 75, 125, 175 and 209 kJ/mol. As discussed earlier, the regeneration enthalpy influences the trade-off between heat transfer requirement and heat pump efficiency.
2. Regeneration pressure was investigated at the levels of 0.032, 0.1, 0.2, 0.3 and 0.368 bar. Lower regeneration pressures (larger pressure swings) will allow for smaller temperature swings and higher heat pump efficiencies.
3. Cycle time was investigated at the levels of 165, 250, 375, 500 and 585 s. Longer cycle times require a larger swing in the degree of sorbent carbonation/regeneration, thus requiring a larger temperature and/or pressure swing. As a trade-off, this increase in sorbent working capacity reduces the sensible heat transfer required per unit CO_2 adsorbed, lowering the load on the heat pump.

As a first indication, an analysis of variance is performed on the results from the central composite design. The second order model is fit to the data and the influence of different model terms (effects) is quantified. Equation 3 shows the model equation for the energy penalty (EP) [%-points relative to benchmark] as a function of the regeneration enthalpy (dH) [kJ/mol], the regeneration pressure (P_{reg}) [bar] and the cycle time (t_{cycle}) [s]. The best fit was achieved with the following coefficients: $x_1 = 15.86, x_2 = -1.221 \times 10^{-1}, x_3 = 4.517 \times 10^{-4}, x_4 = 35.90, x_5 = -11.18, x_6 = -1.005 \times 10^{-2}, x_7 = 6.872 \times 10^{-6}, x_8 = -1.150 \times 10^{-1}, x_9 = 4.080 \times 10^{-5}, x_{10} = -2.320 \times 10^{-2}$.

$$EP = x_1 + x_2 dH + x_3 dH^2 + x_4 P_{reg} + x_5 P_{reg}^2 + x_6 t_{cycle} + x_7 t_{cycle}^2 + x_8 dH P_{reg} + x_9 dH t_{cycle} + x_{10} P_{reg} t_{cycle} \quad \text{Equation 3}$$

As shown in Table 1, the second order model fits the data reasonably well with only 15.3% of the variance in the energy penalty not being explained by the model. Most of the variance in the data is explained by linear effects of the regeneration enthalpy and pressure, and a quadratic effect of the regeneration enthalpy. Some variance is also explained by a linear effect of the cycle time and an interaction effect between regeneration enthalpy and pressure.

Table 1: Analysis of variance (ANOVA) results for the response of the overall SARC energy penalty to changes in the three factors considered. Linear effects are indicated by L and quadratic effects by Q.

Effect	Sum of squares (%)	P-value
Regeneration enthalpy (L)	16.40	0.0443
Regeneration enthalpy (Q)	23.98	0.0220
Regeneration pressure (L)	19.32	0.0331
Regeneration pressure (Q)	0.01	0.9484
Cycle time (L)	8.05	0.1259
Cycle time (Q)	0.13	0.8298
Enthalpy-Pressure interaction	5.92	0.1783
Enthalpy-Time interaction	2.28	0.3812
Pressure-Time interaction	2.43	0.3666

Unexplained variance	15.29

Only the three most influential effects can strictly be considered as statistically significant (p-value < 0.05). The p-value indicates the probability that an observed effect is purely random, so even the linear effect of cycle time (12.6% probability of being random) and the enthalpy-pressure interaction effect (17.8% probability of being random) appear to indicate meaningful trends in the data.

Better insight can be gained from the response surfaces displayed in Figure 9. As could be deduced from the ANOVA, the regeneration enthalpy is the most prominent factor in this analysis. In line with the results from previous section, a curved response is observed with a minimum at intermediate regeneration enthalpies. In general, the energy penalty is greater at the extreme of low regeneration enthalpies than at the extreme of high regeneration enthalpies.

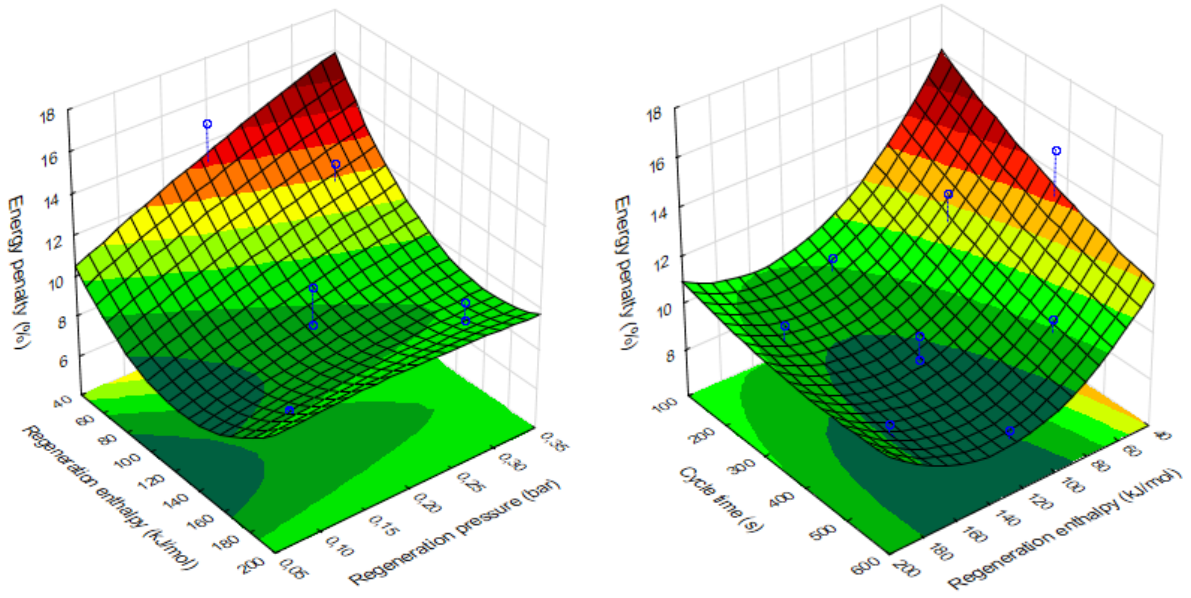

Figure 9: The response of the energy penalty to changes in the three factors under consideration. Blue dots represent the simulated cases.

The second most influential factor, the regeneration pressure, shows a clear tendency towards lower energy penalties at lower regeneration pressures (greater pressure swing). This trend continues beyond the 0.1 bar regeneration pressure used in the previous sections, although it may be impractical and/or uneconomical to draw such strong vacuums in the SARC process because the vacuum pump will become very large. Although not strictly statistically significant, a linear decrease of the energy penalty with increasing cycle times is also clearly observed. Even though this effect is relatively weak, longer cycle times will be preferred from a practicality point of view because the frequency of switching of the inlet and outlet valves will be reduced.

Another perspective is given by plotting response surfaces at the four different regeneration enthalpies investigated in previous sections. As Figure 10 shows, there is a gradual flattening of the response surface as the regeneration enthalpy is increased. At low regeneration enthalpies, the required temperature swing is large, leading to a low heat pump efficiency and large sensible heat transfer requirements. Thus, a large pressure swing (which reduces the required temperature swing) and a longer stage time (which reduces the sensible heat requirement) both have large positive effects

on process efficiency. When the regeneration enthalpy becomes large, however, the required temperature swing is small in all cases, nullifying these positive effects of larger pressure swings and longer stage times.

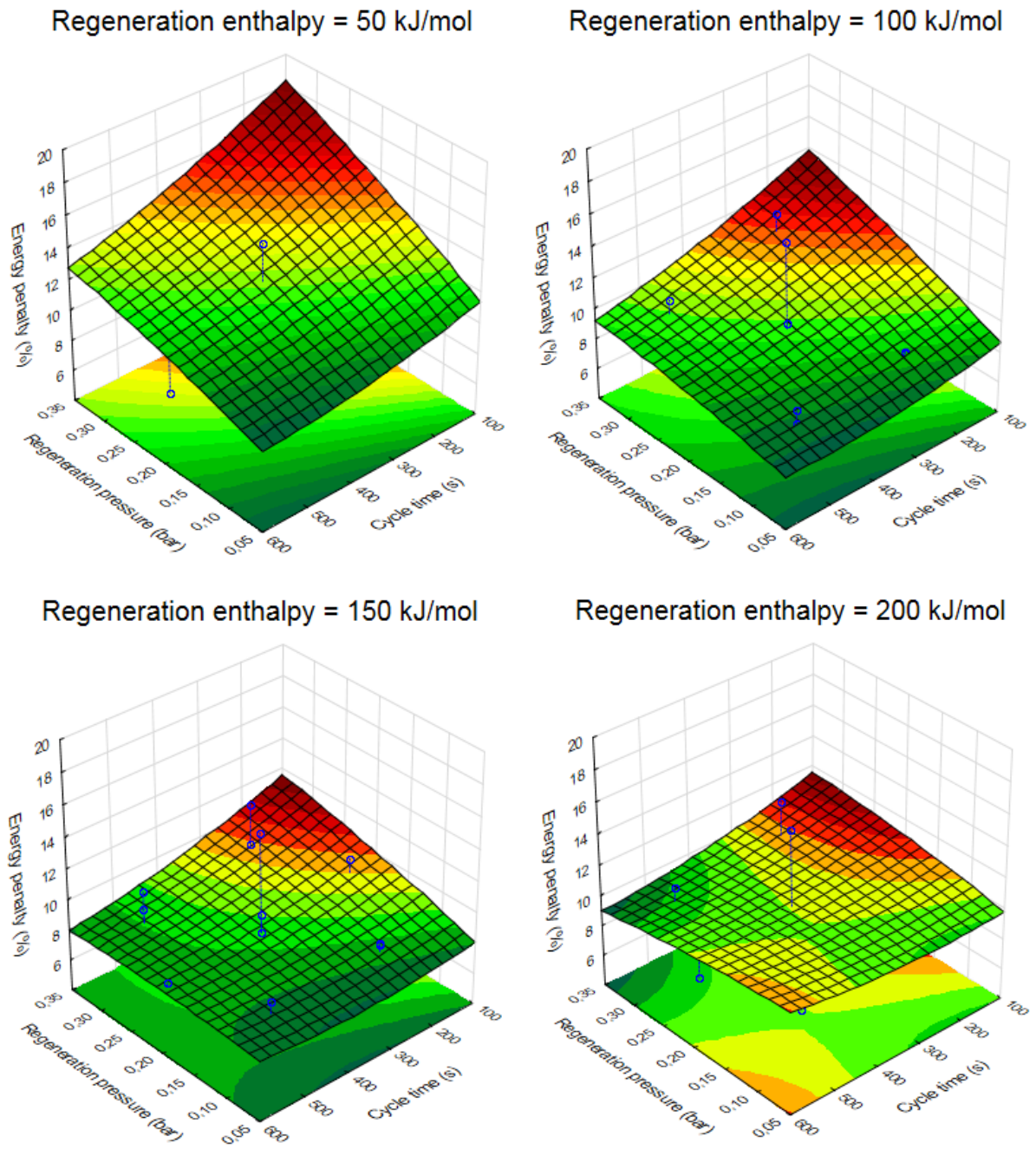

Figure 10: Response of the energy penalty to changes in the regeneration pressure and cycle time for the four different regeneration enthalpies investigated in this work. Blue dots represent the simulated cases.

Figure 10 also shows once more that the energy penalty is generally smallest at intermediate sorbent regeneration enthalpies. If a vacuum of significantly less than 0.1 bar could be drawn, the optimal sorbent regeneration enthalpy could shift lower, but this may not be possible in practice. As a final illustration, the optimal energy penalty is calculated from the second order model fitted through the data for each regeneration enthalpy within a 0.1-0.4 bar range for regeneration pressure and a 150-600 s range for cycle time.

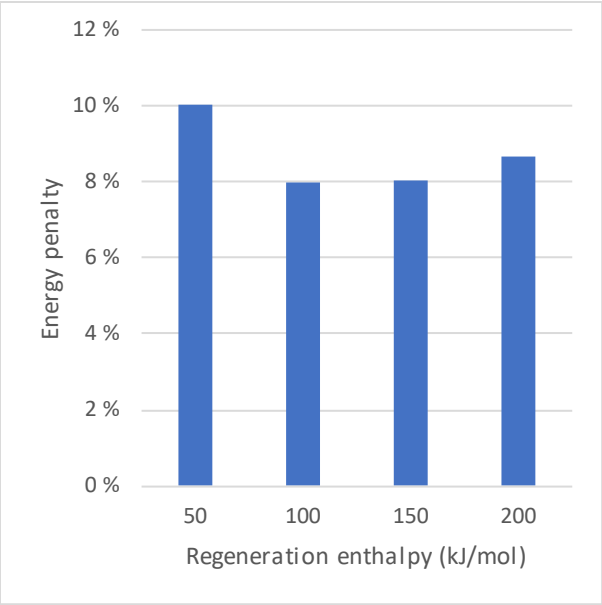

Figure 11: Optimal energy penalty for the four different regeneration enthalpies.

The optimal energy penalties shown in Figure 11 were found under the following regeneration pressures and cycle times: 50 kJ/mol – 0.1 bar and 600 s; 100 kJ/mol – 0.1 bar and 600 s; 150 kJ/mol – 0.1 bar and 450 s; 200 kJ/mol – 0.4 bar and 600 s.

3.5 Comparison to benchmark technologies

The lowest energy penalty achieved by SARC (~8 %-points) is competitive with conventional solvent-based absorption technologies. Optimized process integration with advanced solvents yields an energy penalty of about 9 %-points [5]. Other solvent-based systems impose higher energy penalties up to 12 %-points [3, 4]. However, systems based on piperazine can achieve a lower energy penalty than SARC of about 7.2 %-points [26, 27]. The main benefit of SARC relative to these solvent-based systems is the low degree of integration with the steam cycle, making it a good candidate for retrofits.

When considering sorbent-based systems using multistage fluidized beds, a highly integrated process using multiple sorbent systems operating at different temperatures yielded a minimum energy penalty of 9.5 %-points [10]. Another sorbent-based multistage fluidized bed study [28] reported energy demand similar to amine solvent systems, presumably around 10 %-points.

The calcium looping post-combustion process can better the efficiency of SARC, with penalties indicatively between 6 and 8 %-points, according to the literature [29, 30]. Compared to calcium looping, the main benefit of SARC is that it is expected to be less capital intensive, not requiring an air separation unit and an additional steam power plant for heat recovery.

As quantified in the previous work [17], the SARC concept has a large footprint: a little more than 2x that of an MEA system. However, the SARC reactors will be shorter than a typical MEA absorption column, potentially resulting in competitive reactor capital costs. A future economic assessment study will quantify this aspect. When compared to pure pressure swing adsorption, however, the SARC footprint is 8x smaller, while the energy penalty is also significantly lower than the 10.3 %-points reported in Riboldi and Bolland [31].

The vacuum pump is an important potential capital cost driver of the SARC concept. Webley [32] reported that extreme vacuums will be difficult to achieve due to the large required equipment sizes and associated scalability concerns. For this reason, they recommended future work on concepts capable of achieving good performance at vacuum levels of 0.2-0.3 bar. This aspect will be an important element of planned techno-economic assessment studies of the SARC process. For the time being, it is noted that the minimum energy penalty achieved in this study will increase by about 0.3 %-points if the minimum achievable vacuum is increased from 0.1 to 0.2 bar.

4 Summary and conclusions

The recently proposed SARC concept has the potential to reduce the energy penalty of post-combustion CO_2 capture and simplify the retrofitting of existing power plants or industrial processes. The use of a heat pump to transfer heat from carbonation to regeneration presents an interesting trade-off with respect to regeneration enthalpy of the sorbent. Higher regeneration enthalpies will require more heat transfer, but also allow for a lower temperature difference between carbonation and regeneration, thus enhancing heat pump efficiency.

This trade-off was investigated using a hypothetical CO_2 adsorption isotherm formulated according to the Langmuir model with four different regeneration enthalpies ranging from 50 kJ/mol to 200 kJ/mol. Results showed that intermediate regeneration enthalpies in the range of 100-150 kJ/mol returned the lowest energy penalty, thus clearly illustrating that the SARC concept does not require novel sorbents with very low regeneration enthalpies like other post-combustion concepts. Existing sorbents with relatively high adsorption enthalpies can be used with a high process efficiency.

Employing a taller reactor to increase the heat transfer surface area lowered the energy penalty from the heat pump, but increased the energy penalty from the reactor pressure drop. These two effects cancelled out almost exactly, but the optimum process efficiency shifted towards higher regeneration enthalpies due to the larger capacity to transfer a larger amount of heat between reactors. Nevertheless, the taller reactor did not significantly improve process efficiency and the increased investment cost of such a reactor will therefore not be justified.

Subsequently, water vapour adsorption was included in the simulations. The additional heat of water vapour adsorption is a significant challenge to other post-combustion concepts, but the SARC concept can benefit from the release of water vapour under regeneration to reduce the CO_2 partial pressure, thus reducing the required temperature swing and increasing the heat pump efficiency. Simulation results showed that the optimal energy penalty remained similar between the cases with and without water vapour adsorption, illustrating that this is not a problem for the SARC concept.

Finally, a central composite design was completed to gain a more complete understanding of the behaviour of sorbents with different regeneration enthalpies in the SARC concept. For low regeneration enthalpies, process efficiency increases significantly with a higher pressure swing (which reduces the large temperature swing required) and larger degrees of sorbent utilization (which reduces the large sensible heat transfer associated with large temperature swings). For high regeneration enthalpies, on the other hand, the process efficiency was insensitive to these two variables. These results will be very useful in future studies of sorbent selection for the SARC concept.

5 Acknowledgement

This study was performed as part of the project entitled "Demonstration of the Swing Adsorption Reactor Cluster (SARC) for simple and cost effective post-combustion CO_2 capture", funded by the Research Council of Norway under the CLIMIT program (grant no. 268507/E20).

6 References

1. UNFCCC. *Historic Paris Agreement on Climate Change*. United Nations Framework Convention on Climate Change 2015; Available from: http://newsroom.unfccc.int/unfccc-newsroom/finale-cop21/.
2. IPCC, *Fifth assessment report: Mitigation of climate change*. 2014, Intergovernmental panel on Climate Change.
3. Rubin, E.S., J.E. Davison, and H.J. Herzog, *The cost of CO2 capture and storage.* International Journal of Greenhouse Gas Control, 2015. **40**: p. 378-400.
4. Ahn, H., et al., *Process configuration studies of the amine capture process for coal-fired power plants.* International Journal of Greenhouse Gas Control, 2013. **16**: p. 29-40.
5. Kvamsdal, H.M., et al., *Optimizing integrated reference cases in the OCTAVIUS project.* International Journal of Greenhouse Gas Control, 2016. **50**: p. 23-36.
6. Samanta, A., et al., *Post-Combustion CO2 Capture Using Solid Sorbents: A Review.* Industrial & Engineering Chemistry Research, 2012. **51**(4): p. 1438-1463.
7. Shen, C., et al., *Two-Stage VPSA Process for CO2 Capture from Flue Gas Using Activated Carbon Beads.* Industrial & Engineering Chemistry Research, 2012. **51**(13): p. 5011-5021.
8. Wang, L., et al., *CO2 capture from flue gas by two successive VPSA units using 13XAPG.* Adsorption, 2012. **18**(5): p. 445-459.
9. Lee, J.B., et al., *CO2 capture from flue gas using potassium-based dry regenerable sorbents.* Energy Procedia, 2011. **4**: p. 1494-1499.
10. Kim, K., et al., *A solid sorbent-based multi-stage fluidized bed process with inter-stage heat integration as an energy efficient carbon capture process.* International Journal of Greenhouse Gas Control, 2014. **26**: p. 135-146.
11. Yi, C.-K., et al., *Continuous operation of the potassium-based dry sorbent CO2 capture process with two fluidized-bed reactors.* International Journal of Greenhouse Gas Control, 2007. **1**(1): p. 31-36.
12. Veneman, R., et al., *Continuous CO2 capture in a circulating fluidized bed using supported amine sorbents.* Chemical Engineering Journal, 2012. **207–208**: p. 18-26.
13. Proell, T., et al., *Introduction and evaluation of a double loop staged fluidized bed system for post-combustion CO2 capture using solid sorbents in a continuous temperature swing adsorption process.* Chemical Engineering Science, 2016. **141**: p. 166-174.
14. Roy, S., C.R. Mohanty, and B.C. Meikap, *Multistage Fluidized Bed Reactor Performance Characterization for Adsorption of Carbon Dioxide.* Industrial & Engineering Chemistry Research, 2009. **48**(23): p. 10718-10727.
15. Zanco, S.E., et al., *Modeling of Circulating Fluidized Beds Systems for Post-Combustion CO2 Capture via Temperature Swing Adsorption.* Aiche Journal, 2018. **64**(5): p. 1744-1759.
16. Kim, K., et al., *Moving bed adsorption process with internal heat integration for carbon dioxide capture.* International Journal of Greenhouse Gas Control, 2013. **17**: p. 13-24.
17. Zaabout, A., et al., *Thermodynamic assessment of the swing adsorption reactor cluster (SARC) concept for post-combustion CO2 capture.* International Journal of Greenhouse Gas Control, 2017. **60**(Supplement C): p. 74-92.
18. Goto, K., K. Yogo, and T. Higashii, *A review of efficiency penalty in a coal-fired power plant with post-combustion CO2 capture.* Applied Energy, 2013. **111**: p. 710-720.

19. Oexmann, J. and A. Kather, *Minimising the regeneration heat duty of post-combustion CO2 capture by wet chemical absorption: The misguided focus on low heat of absorption solvents.* International Journal of Greenhouse Gas Control, 2010. **4**(1): p. 36-43.
20. van Nierop, E.A., et al. *Effect of absorption enthalpy on temperature-swing CO2 separation process performance*. in *GHGT-9*. 2011.
21. Park, Y.C., et al., *Long-term operation of carbon dioxide capture system from a real coal-fired flue gas using dry regenerable potassium-based sorbents.* Energy Procedia, 2009. **1**(1): p. 1235-1239.
22. Park, S.-W., et al., *Carbonation kinetics of potassium carbonate by carbon dioxide.* Journal of industrial and engineering chemistry, 2006. **12**(4): p. 522-530.
23. Nelson, T.O., et al., *The dry carbonate process: Carbon dioxide recovery from power plant flue gas.* Energy Procedia, 2009. **1**(1): p. 1305-1311.
24. Veneman, R., et al., *Adsorption of H2O and CO2 on supported amine sorbents.* International Journal of Greenhouse Gas Control, 2015. **41**: p. 268-275.
25. Montgomery, D., *Design and Analysis of Experiments*. 5 ed. 2001, New York: John Wiley and Sons.
26. Kvamsdal, H.M., et al., *Energetic evaluation of a power plant integrated with a piperazine-based CO2 capture process.* International Journal of Greenhouse Gas Control, 2014. **28**: p. 343-355.
27. Van Wagener, D.H., et al., *Maximizing coal-fired power plant efficiency with integration of amine-based CO2 capture in greenfield and retrofit scenarios.* Energy, 2014. **72**: p. 824-831.
28. Pröll, T., et al., *Introduction and evaluation of a double loop staged fluidized bed system for post-combustion CO2 capture using solid sorbents in a continuous temperature swing adsorption process.* Chemical Engineering Science, 2016. **141**: p. 166-174.
29. Perejón, A., et al., *The Calcium-Looping technology for CO2 capture: On the important roles of energy integration and sorbent behavior.* Applied Energy, 2016. **162**: p. 787-807.
30. Martínez, I., et al., *Review and research needs of Ca-Looping systems modelling for post-combustion CO2 capture applications.* International Journal of Greenhouse Gas Control, 2016. **50**: p. 271-304.
31. Riboldi, L. and O. Bolland, *Evaluating Pressure Swing Adsorption as a CO2 separation technique in coal-fired power plants.* International Journal of Greenhouse Gas Control, 2015. **39**: p. 1-16.
32. Webley, P.A., *Adsorption technology for CO2 separation and capture: a perspective.* Adsorption, 2014. **20**(2): p. 225-231.

Appendix

Note that all energy penalties and SPECCA values are calculated relative to the reference plant without CO_2 capture assessed in the previous work [17]. This plant has an electrical efficiency of 44.57% and specific emissions of 782.1 kg/MWh. All SARC plants achieve 90% CO_2 capture and 96% CO_2 purity.

Table A 1: Main results of power plants simulations in 5 m reactor case with no water vapour adsorption (Figure 5).

Regeneration enthalpy (kJ/mol)	**200**	**150**	**100**	**50**
Steam cycle net power output (MW)	770.5	770.9	770.9	779.1
Power consumption (MW)				
Forced draft fans	3.4	3.4	3.4	3.4
Induced draft fan	9.9	9.9	9.9	9.9
Adsorption reactor fan	11.2	11.2	11.2	11.2
Regeneration reactor fan	0.4	0.4	0.4	0.4
Heat pump compressor	57.0	46.8	48.0	116.1

Regeneration vacuum pump	28.5	28.5	28.5	28.5
Evacuation vacuum pump	1.9	1.8	1.7	0.9
CO_2 compression	53.9	53.9	53.9	53.9
Coal milling and handling	3.3	3.3	3.3	3.3
Ash handling	1.9	1.9	1.9	1.9
Flue gas desulphurization	3.3	3.3	3.3	3.3
Auxiliaries for heat rejection	0.9	0.8	0.8	1.0
Balance of plant	2.5	2.5	2.5	2.5
Net power (MW)	592.6	603.4	602.2	543.0
Efficiency (%)	35.76	36.41	36.34	32.77
Energy penalty (%)	-8.81	-8.16	-8.23	-11.80
Specific emissions (kg/MWh)	97.86	96.10	96.29	106.80
SPECCA ($MJ_{LHV}/kgCO_2$)	2.91	2.64	2.67	4.31

Table A 2: Main results of power plants simulations in 10 m reactor case with no water vapour adsorption (Figure 6).

Regeneration enthalpy (kJ/mol)	**200**	**150**	**100**	**50**
Steam cycle net power output (MW)	771.2	771.4	771.1	778.8
Power consumption (MW)				
Forced draft fans	3.4	3.4	3.4	3.4
Induced draft fan	9.9	9.9	9.9	9.9
Adsorption reactor fan	22.9	22.9	22.9	22.9
Regeneration reactor fan	0.4	0.4	0.4	0.4
Heat pump compressor	39.2	36.6	43.1	111.3
Regeneration vacuum pump	28.5	28.5	28.5	28.5
Evacuation vacuum pump	2.4	2.2	1.7	0.6
CO_2 compression	53.9	53.9	53.9	53.9
Coal milling and handling	3.3	3.3	3.3	3.3
Ash handling	1.9	1.9	1.9	1.9
Flue gas desulphurization	3.3	3.3	3.3	3.3
Auxiliaries for heat rejection	0.7	0.6	0.7	0.9
Balance of plant	2.5	2.5	2.5	2.5
Net power (MW)	599.1	602.0	595.7	536.1
Efficiency (%)	36.16	36.33	35.95	32.35
Energy penalty (%)	-8.41	-8.24	-8.62	-12.22
Specific emissions (kg/MWh)	96.79	96.32	97.35	108.16
SPECCA ($MJ_{LHV}/kgCO_2$)	2.74	2.67	2.83	4.53

Table A 3: Main results of power plants simulations in 5 m reactor case with water vapour adsorption (Figure 8).

Regeneration enthalpy (kJ/mol)	**200**	**150**	**100**	**50**
Steam cycle net power output (MW)	770.7	771.3	771.6	770.9
Power consumption (MW)				
Forced draft fans	3.4	3.4	3.4	3.4

Induced draft fan	9.9	9.9	9.9	9.9
Adsorption reactor fan	11.2	11.2	11.2	11.2
Regeneration reactor fan	0.6	0.6	0.6	0.7
Heat pump compressor	52.6	38.0	31.4	49.3
Regeneration vacuum pump	39.8	39.9	40.1	40.6
Evacuation vacuum pump	2.5	2.5	2.5	1.5
CO_2 compression	53.9	53.9	53.9	53.9
Coal milling and handling	3.3	3.3	3.3	3.3
Ash handling	1.9	1.9	1.9	1.9
Flue gas desulphurization	3.3	3.3	3.3	3.3
Auxiliaries for heat rejection	1.8	1.7	1.7	1.9
Balance of plant	2.5	2.5	2.5	2.5
Net power (MW)	584.1	599.3	606.1	587.6
Efficiency (%)	35.25	36.17	36.58	35.46
Energy penalty (%)	-9.32	-8.40	-7.99	-9.11
Specific emissions (kg/MWh)	99.27	96.76	95.67	98.69
SPECCA ($MJ_{LHV}/kgCO_2$)	3.13	2.74	2.57	3.04

Table A 4: Main results of power plants simulations in the central composite design (Table 1 and Figure 9).

Regeneration enthalpy (kJ/mol)	**75**	**75**	**75**	**75**	**175**	**175**	**175**	**175**	**40.9**	**209.1**	**125**	**125**	**125**	**125**	**125**
Regeneration pressure (bar)	**0.1**	**0.1**	**0.3**	**0.3**	**0.1**	**0.1**	**0.3**	**0.3**	**0.2**	**0.2**	**0.0318**	**0.3682**	**0.2**	**0.2**	**0.2**
Cycle time (s)	**250**	**500**	**250**	**500**	**250**	**500**	**250**	**500**	**375**	**375**	**375**	**375**	**164.8**	**585.2**	**375**
Steam cycle net power output (MW)	771.2	771.6	780.3	769.1	771.0	771.0	769.1	769.7	781.8	769.7	773.1	769.3	769.4	770.6	770.5
Power consumption (MW)															
Forced draft fans	3.4	3.4	3.4	3.4	3.4	3.4	3.4	3.4	3.4	3.4	3.4	3.4	3.4	3.4	3.4
Induced draft fan	9.9	9.9	9.9	9.9	9.9	9.9	9.9	9.9	9.9	9.9	9.9	9.9	9.9	9.9	9.9
Adsorption reactor fan	11.2	11.2	11.2	11.2	11.2	11.2	11.2	11.2	11.2	11.2	11.2	11.2	11.2	11.2	11.2
Regeneration reactor fan	0.6	0.6	0.7	0.6	0.6	0.6	0.6	0.6	0.7	0.6	0.6	0.6	0.6	0.6	0.6
Heat pump compressor	42.4	32.4	142.0	94.0	44.4	45.6	88.1	76.6	176.0	75.7	6.9	86.5	81.4	56.2	58.7
Regeneration vacuum pump	40.4	40.2	16.4	17.0	39.8	39.8	17.0	17.0	23.8	25.2	67.4	13.6	25.2	25.2	25.2
Evacuation vacuum pump	4.2	2.0	4.1	2.0	4.8	1.5	4.6	1.5	1.3	2.4	2.6	2.5	8.3	1.4	2.5
CO_2 compression	53.9	53.9	53.9	53.9	53.9	53.9	53.9	53.9	53.9	53.9	53.9	53.9	53.9	53.9	53.9
Coal milling and handling	3.3	3.3	3.3	3.3	3.3	3.3	3.3	3.3	3.3	3.3	3.3	3.3	3.3	3.3	3.3
Ash handling	1.9	1.9	1.9	1.9	1.9	1.9	1.9	1.9	1.9	1.9	1.9	1.9	1.9	1.9	1.9
Flue gas desulphurization	3.3	3.3	3.3	3.3	3.3	3.3	3.3	3.3	3.3	3.3	3.3	3.3	3.3	3.3	3.3
Auxiliaries for heat rejection	1.8	1.7	1.9	2.0	1.7	1.8	1.8	1.6	2.4	1.8	1.9	1.7	2.0	1.6	1.7
Balance of plant	2.5	2.5	2.5	2.5	2.5	2.5	2.5	2.5	2.5	2.5	2.5	2.5	2.5	2.5	2.5
Net power (MW)	592.5	605.5	525.8	564.1	590.3	592.4	567.7	583.1	488.4	574.7	604.3	575.1	562.6	596.3	592.6
Efficiency (%)	35.75	36.54	31.73	34.04	35.62	35.75	34.26	35.19	29.47	34.68	36.47	34.70	33.95	35.98	35.76
Energy penalty (%)	-8.82	-8.03	-12.84	-10.53	-8.95	-8.82	-10.31	-9.38	-15.10	-9.89	-8.10	-9.87	-10.62	-8.59	-8.81
Specific emissions (kg/MWh)	97.88	95.77	110.28	102.80	98.23	97.88	102.14	99.45	118.74	100.90	95.96	100.84	103.06	97.25	97.86
SPECCA ($MJ_{LHV}/kgCO_2$)	2.91	2.59	4.86	3.68	2.97	2.91	3.57	3.15	6.24	3.38	2.62	3.37	3.72	2.81	2.91